ORIGINAL ARTICLE

Sea-level change and human occupation over 6000 years on Areoso Island (Ría de Arousa, NW Iberian Peninsula)

Daniel Cajade-Pascual[1] · Manuela Costa-Casais[1] · Ramón Blanco-Chao[1] · Teresa Taboada Rodríguez[2]

Abstract

Coastal areas are extremely sensitive to variations in environmental conditions. The interaction of marine and continental processes causes a high degree of dynamism, generating depositional formations of great value for palaeoenvironmental reconstruction. This paper focuses on two pedostratigraphic deposits located under the current beach, in close proximity to archaeological tumuli located on Areoso Island (Ría de Arousa, NW Iberian Peninsula). Employing a geoarchaeological approach, sea-level rise, environmental conditions and human occupation over a 6000-year period are interpreted. The results of granulometric and mineralogical data, elemental composition and stratigraphic features, help to identify three successive environments: continental (rock weathering, soil formation and erosion); a transition to a coastal environment; and the establishment of full coastal conditions. The geomorphological evolution of the last 6.0 kyr BP has been controlled by climate, sea-level rise and human activity. The continental facies shows evidence of low sea-level up to 4.8 kyr BP and the first evidence of coastal processes after 3.2 kyr BP. These pedostratigraphic deposits located in an open coastal system improve the Holocene sea-level rise curve in the NW Iberian Peninsula and help to understand the context in which the most important archaeological structures on the island (the tumuli) began to be eroded.

Keywords Pedostratigraphic sequences · Sea-level change · Geoarchaeology · NW Iberian Peninsula

Introduction

Interest in the study of past environmental changes has significantly increased over recent decades, deriving from concern about future scenarios in the context of global change. As the interface between continent and sea, coastal systems are highly sensitive to environmental changes.

✉ Daniel Cajade-Pascual
  danielcajade.pascual@usc.es

  Manuela Costa-Casais
  manuela.costa@usc.es

  Ramón Blanco-Chao
  ramon.blanco@usc.es

  Teresa Taboada Rodríguez
  teresa.taboada@usc.es

[1] Department of Geography, University of Santiago de Compostela, Praza da Universidade, 1, 15782 Santiago de Compostela, Spain

[2] Department of Pedology and Agricultural Chemistry, University of Santiago de Compostela, Campus Vida s/n, 15782 Santiago de Compostela, Spain

Indeed, their dynamism makes them highly valuable places for palaeoenvironmental reconstruction. Scientific research of coastal palaeoenvironmental conditions and sea-level changes during the Holocene in the NW of the Iberian Peninsula have been conducted in lagoons (e.g.,Bao et al. 2007; Costas et al. 2009; González-Villanueva et al. 2015; Sáez et al. 2018), estuaries (e.g.,Granja et al. 2022; Leorri et al. 2013), coastal sedimentary deposits (e.g.,Álvarez-Alonso et al. 2020; Blanco-Chao et al. 2019; Costa-Casais et al. 2012b; Feal-Pérez et al. 2014; Gómez-Orellana et al. 2021) and in sea-floor sediments (e.g.,Andrade et al. 2011, 2014; Cartelle et al. 2022; García-Moreiras et al. 2019; Muñoz Sobrino et al. 2022). Although these studies provide a general overview of the environmental conditions during the Holocene and changes in sea-level, there is still much to be learned about the detailed evolution of the coast. The rising Holocene sea-level caused the development of sand barriers, coastal lagoons, beach-dune systems and estuarine prisms (Alonso and Pagés 2010; Sáez et al. 2018). In a lagoon complex, González-Villanueva et al. (2015) identified a phase of retrogradation of the dune barrier between 5.3 and 3.5 kyr BP, followed by a period of barrier breaching

🖄 Springer

and overwashing between 3.5 and 1.5 kyr BP. This phase of dune barrier breaching was also detected on Cíes Islands by Costas et al. (2009) at around 3.7 kyr BP. The available data suggest that the present-day sea-level was not reached before 4.0–3.5 kyr BP (Bao et al. 2007; Costas et al. 2009; González-Villanueva et al. 2015). Most of these studies were conducted on sediments from lagoons, a type of coastal system from which uncertainties can arise due to their specific hydrodynamics (Fruergaard et al. 2011) and human impact (Sáez et al. 2018). The Holocene marine transgression caused significant changes in coastal systems, which have been adapting to rising sea levels until reaching the present level. These changes have not only been driven by natural forcing, as human impact during the Holocene has also played a significant role, especially since the Neolithic (Benjamin et al. 2017; David et al. 2022). This fact confers great interest upon coastal archaeological sites, many of which are currently endangered by rising sea levels and human interference (Erlandson 2012; Fitzpatrick et al. 2015). The objective of this study is to reconstruct the environmental evolution of Areoso Island since the Middle Holocene, using the information stored in soils and sediments and focusing on sea-level rise and the human occupation of the island.

Study area

The north-western coast of the Iberian Peninsula is a rough and indented coastline developed on the plutonic and metamorphic rocks of the Iberian Massif (Variscan orogeny). Tectonic activity has been detected during the Quaternary (Martínez-Carreño and García-Gil 2017), although the coast has remained stable since the Upper Pleistocene (Blanco-Chao et al. 2003). The genesis of the Galician rias lies in the tectonic modelling of the rocky bed since the Eocene and excavation during the last glaciation or glaciations (Martínez-Carreño and García-Gil 2017). The Ría de Arousa, on the Atlantic coast of NW Spain, is the largest of all the Galician rias and has an NW–SE-oriented central axis. During the marine regression of the last Glacial period, with a global sea-level 130 m below that of the present (Lambeck et al. 2014), this ria was a fluvial valley dominated by continental processes. In the initial phases of postglacial transgression and the Early Holocene, a tidal estuary was established and, as the valley was flooded by the sea, the influence of the tides decreased in favour of wave processes (Cartelle et al. 2022). Since 7.0 kyr BP, still with a low sea-level (around 7 m below that of the present), there was a significant decrease in rates of transgression (García-Artola et al. 2018). As the sea-level approached its present level, the mouths of the Ulla and Umia rivers receded to their current position, where fluvial sediments are shaped by tidal processes (Cartelle et al. 2022). Today, the ria has

a complex physiography, with bays, peninsulas and islands, in which sandy beaches are interspersed with low rocky areas. In its innermost part is the estuary of the Ulla River. The O Grove peninsula and the island of Sálvora are natural closures that separate the ria from the open ocean, dissipating wave energy, which can be considered to be low in the inner part of the ria. Although no direct data is available from inside the ria, the characterisation of the wave regime can be derived from the open ocean data set (SIMAR point 1043070), which shows that 70% of the waves are between 1 and 2.5 m of significant height (Hs) and occur at periods of between 8 and 10 s. Maximum Hs in autumn and winter can reach 14 m. 73% of the open ocean waves approach from NNW to WNW, 14% from WSW and 9% arrive from the WSW and SW. In the Vilagarcía tidal gauge, located at a distance of 12 km from Areoso Island, the mean spring tidal range is 3.45 m and the maximum astronomical tidal range is 4.22 m (Spanish Port Authority 2017).

Areoso is a small island, forming part of a shoal in the inner part of the Ría de Arousa, located to the west of the island of Arousa (Fig. 1). Its northern sector is basically a lobe of sandy, partially phytostabilised, sediment, while the south is a granitic substrate covered by an aeolian mantle. Its northern section is connected to the south via a low narrow isthmus. The bathymetry of the area shows that the Areoso shoal is structurally part of the island of Arousa, which is separated from the continent by a 2–3 km-wide strait with water depths of between 5 and 7 m. To the north, depth increases sharply, with a scarp of 15 m, reaching depths up to 20–25 m. To the west, there is a more pronounced scarp of around 30 m, which corresponds to the southern margin of a palaeovalley channelled in the bottom of the ria.

Archaeological studies have defined Areoso as an exceptional archaeological site due to the fact that it is unusual to find prehistoric funerary monuments from the Neolithic and Bronze Age in the low-lying coastal areas of the NW Iberian Peninsula (López-Romero et al. 2015; Mañana-Borrazás et al. 2020; Rey García 2011). Some of the most outstanding archaeological sites remained hidden by thick aeolian sediments until the twentieth century, with no evidence of ever having been looted. However, erosion has led to the destruction of some of the prehistoric structures and threatens those that are still preserved. The natural and cultural heritage of Areoso is at risk from high erosion rates, particularly in its western sector, where the dune front has regressed by up to 60 m since the 1980s (Blanco-Chao et al. 2020).

Materials and methods

During an archaeological intervention in September 2015, four archaeological test pits were opened in an area, where two funerary tumuli are located, a prominent archaeological
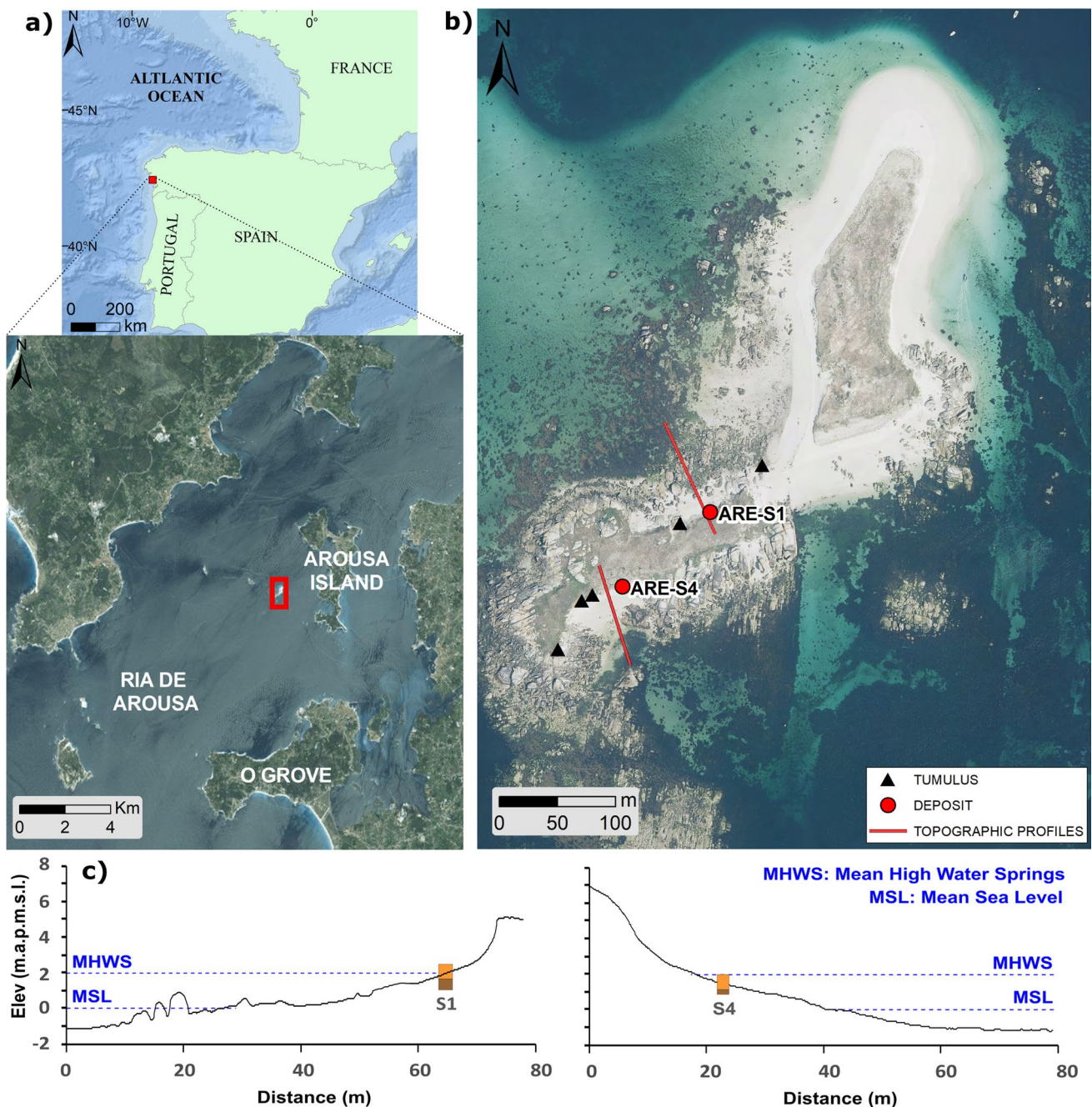
Fig. 1 **a** Location of Areoso Island inside the Ría de Arousa. **b** Location of the two sedimentary deposits. **c** Topographic profiles with the elevation of the pedostratigraphic deposits in relation to the present mean sea-level (MSL) and mean high water spring level (MHWS)

site on the island (Chao-Álvarez 2015). The two deeper pits, ARE-S1 and ARE-S4 (referred to here as S1 and S4), were selected for sampling and characterisation of the soils and sediments, and the environment in which they formed (Figs. 1, 2).

Stratigraphic and morphological data were collected in the field according to the criteria established in the Guidelines for Soil Description (FAO 2009). Samples were taken in the two open columns every 5 cm from top to bottom.

One column located on the western flank of the island (S1) reached a depth of 140 cm from the surface of the present-day beach with a total of 28 samples. The other deposit on the eastern flank has a thickness of 110 cm and 23 samples. The elevation of the two deposits was obtained using a centimetric RTK GNSS receiver and referred to the Spanish official vertical datum (Figs. 1, 2).

Each sample was described in the laboratory according to the Guidelines for Soil Description (FAO 2009) in terms

Fig. 2 Archaeological test pits and sample columns

of grain size, structure, consistency, plasticity, sedimentary and soil characteristics, and colour. The samples were air-dried and sieved to separate the coarse fraction (> 2 mm) from the fine earth fraction (< 2 mm). In the fine earth soil reaction, loss on ignition (LOI), elemental and mineralogical composition were determined. Elemental and mineralogical composition was examined on finely milled (< 100 μm) samples. The samples were sieved after previous disaggregation with hydrochloric acid and sodium hexametaphosphate. The amount of silt and clay was calculated by washing the samples in a 0.063 mm sieve. The fraction > 0.063 mm

was sieved with a column of sieves ranging from 0.063 to 2 mm. In this study, gravels comprise particles between 2 and 8 mm, classified as granules and fine pebbles according to the Wentworth scale (Wentworth 1922). The statistical parameters of mean size and sorting were obtained using the method of Folk and Ward (1957) using the Gradistat spreadsheet (Blott and Pye 2001). A morphometric study was carried out on 1 and 0.4 mm fractions of the odd-numbered samples of S1, selecting 100 particles in each fraction for comparison under a stereomicroscope. The determination of biogenic carbonates (shell fragments) was made with

10% diluted hydrochloric acid. Soil reaction was measured in water (pHw) suspensions (1:2.5) with a pH-meter following standard procedures (Guitián and Carballas 1976; Urrutia et al. 1989). The mineralogical study was carried out on all S1 samples by X-ray diffraction with a Philips PW1820. The LOI was determined by calcination of the sample at 550 °C for 6 h. Total C and N contents were measured with a LECO Elemental Analyser, model CNS-2000. Major and minor element concentrations (Si, Al, Fe, Ti, K, Ca, Na, Sr and Zr) were determined by X-ray fluorescence (Cheburkin and Shotyk 1996).

Two samples in each deposit were selected for ^{14}C dating according to: (a) changes in carbon content, which could be indicative of the presence of buried soil cycles; (b) location in the sedimentary deposit and relationship with erosive discontinuities and abrupt changes in texture. The fraction < 2 mm of each of the selected samples was shacked in ultrapure distilled water for 16 h. Then, the suspension was filtered through a sieve of 50 μm mesh-size, to separate sand, roots and fresh organic remains. The resulting suspension was dried in an air heater at a temperature not higher than 35 °C. ^{14}C measurement, using accelerator mass spectrometry, was conducted by Beta Analytic laboratory. The Conventional ^{14}C ages were calibrated using CALIB 8.2 (Stuiver et al. 2021) and are expressed as calibrated years before present (cal. yr BP and BC/AD) (Table 1).

Results

Pedostratigraphic features

The two pedosedimentary deposits studied are characterised by six stratigraphic units (Figs. 2, 3):

I.   *Depth*: 0–20 cm in S1 and 0–45 cm in S4. Colour (wet): greyish-brown. Colour (dry): light greyish-brown. Sandy material without structure in which some fine to medium aggregate is mixed into subangular blocks with slight to moderate structure. Not adherent, not plastic. Features of incipient soil formation processes are present. In S4 a coin dating from 1986 was found at a depth of 35 cm during the archaeological campaign (Chao-Álvarez 2015). The limit with unit II is gradual.

II. *Depth*: 20–40 cm in S1 and 45–55 cm in S4. Colour (W): brown with reddish hue. Colour (D): greyish-brown. Sandy material without structure, in which some small aggregate is mixed into subangular blocks with slight structure. Not adherent, not plastic. The features of pedogenesis are very incipient. Archaeological material (small pottery fragments, of unidentifiable cultural stage) appears in the middle of the layer. In S1, towards the base of this level there are rounded and flattened quartz gravels. The limit with unit III is clear in S1 and gradual in S4.

III. *Depth*: 40–70 cm in S1 and 55–70 cm in S4. Colour (W): brown with reddish hue. Colour (D): greyish-brown. Sandy layer, without structure, not plastic, not adherent. Few pedogenetic features. In S1, towards the base of this level, it mixes with the organic layer that fossilises, filling in small cracks or forming a kind of lamellae. The limit with unit IV is clear in S1 and gradual in S4.

IV. *Depth*: 70–90 cm in S1 and 70–80 cm in S4. Colour (W): blackish-brown. Colour (D): light brown in S1 and brown in S4. Fine material, rich in sand, with a moderate structure in fine to medium subangular blocks mixed with material of a fine granular structure. Slightly adherent and plastic. Pottery remnants have been found and, in the case of S4, charcoal lines are observed. The limit with unit V is gradual in S1 and clear in S4.

V.   *Depth*: 90–120 cm in S1 and 80–110 cm in S4. Colour (W): black. Colour (D): brown. Layer composed of sand, silt and clay mixed with abundant angular granitic gravels and scarce angular quartz. The material is structured in medium to fine subangular blocks mixed with others of a fine granular structure. Slightly adherent and plastic. The limit with unit VI is gradual in S1 and clear in S4.

VI. *Depth*: 120–140 cm in S1 and 110–115 cm in S4. Colour (W): greyish-yellow. Colour (D): light greyish-yellow. Angular granite sands and angular gravels in a fine matrix, corresponding to an in situ weathered granite layer.

Table 1 Calibrated radiocarbon dating on the S1 and S4 stratigraphic deposits

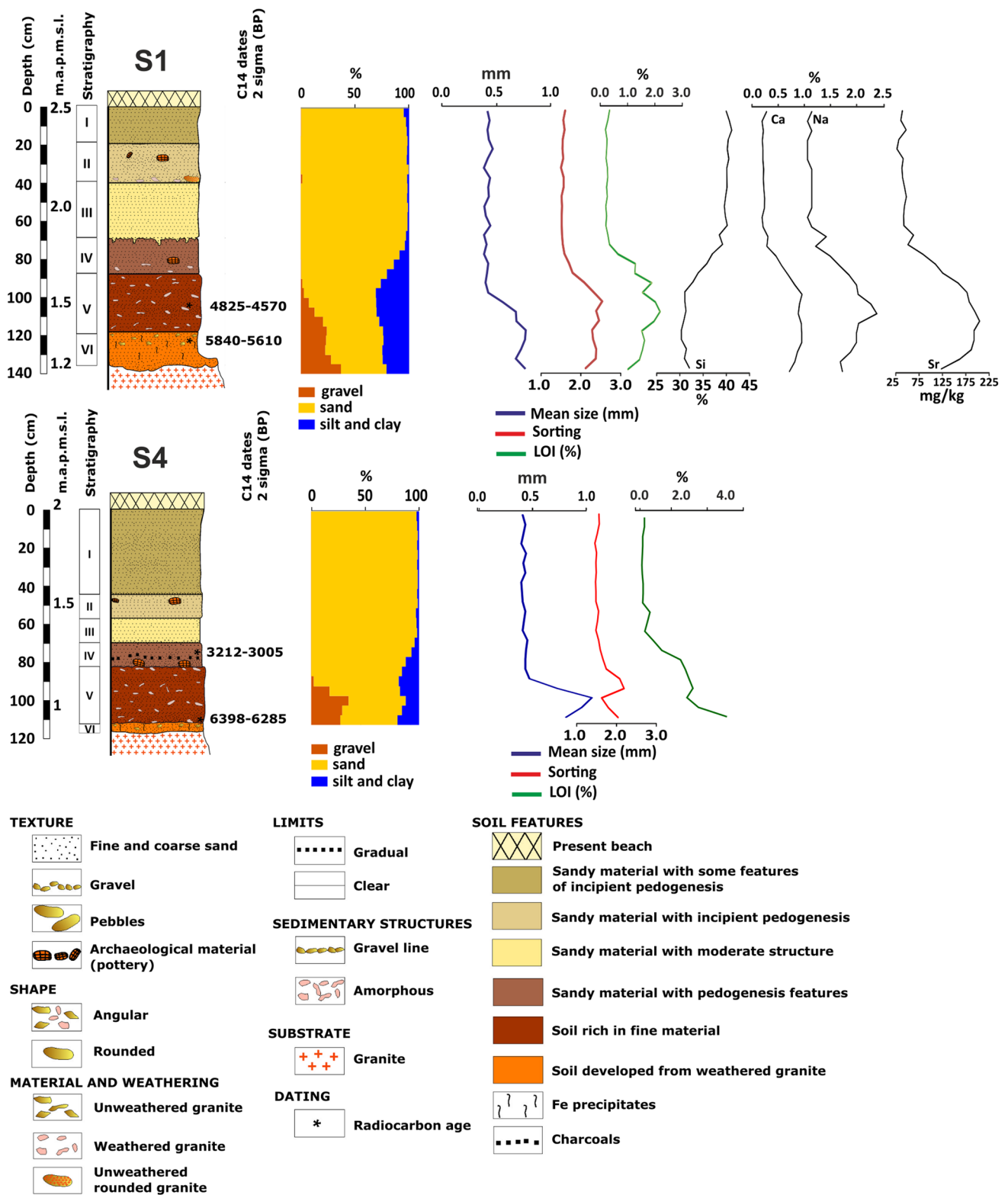| Samples	Lab code	Dating material	Depth (cm)	Age (2σ cal year BP)	Age (BC/AD)	Age (^{14}C yr BP)
S1-22	β449811	Organic sediment	105–110	4825–4570	2875–2620	4697.5 ± 127
S1-25	β449812	Organic sediment	120–125	5840–5610	3890–3660	5725 ± 115
S4-15	β499253	Organic sediment	70–75	3212–3005	1263–1056	3108.5 ± 103
S4-22	β499254	Organic sediment	105–110	6398–6285	4449–4336	6341.5 ± 56

Fig. 3 Sedimentological and geochemical parameters within S1 and S4

Sedimentological, grain-size and morphometry results

The granulometric data of the S1 and S4 deposits allow for the identification of three phases: one basal, which corresponds to stratigraphic units VI and V; one transitional, coinciding with unit IV; and an upper phase, including units III, II and I (Fig. 3). The basal units (VI and V) are developed from granitic substrate and are composed of gravel and medium sand in a silt and clay matrix. In these units, there are angular gravels (decreasing from around 30% at the base to 1% at the top of unit V), sands and silt and clay content with values higher than 20% in S1 and 12% in S4. The upper part of unit V consists of sandier sediments with more than 72% sand (Fig. 3). The mean size of the sand and gravel fractions ranges from 1 to 0.6 mm, decreasing down to 0.4 mm in the upper part of unit V. In general, units VI and V are bimodal poorly sorted sediments with medium sand and gravel in a muddy matrix and abundant feldspar and granite fragments (Fig. 3).

The transition layer (unit IV) is formed mainly by an upwardly increasing content in medium, albeit poorly sorted, sand (up to 79%) with a mean size of 0.4 mm. The gravel and silt and clay content decreases from the base to the top of the unit (Fig. 3 and Online Resource 1).

The upper units (III, II and I) correspond to moderately well-sorted medium sands, with a constant mean size of 0.4 mm throughout the layer. The gravel content does not exceed 1.3% and silt and clay vary between a minimum of 0.3 to a maximum of 4.8% in the upper part (Fig. 3). Morphometrically, this is an immature siliciclastic sediment. Biogenic particles (fragments of shells) are present but with low percentages (less than 2%) in both deposits, with the exception of the two uppermost samples of S4, in which values reach 6.8%. Most of the material is angular or poorly rounded, indicating poor transport from its area of origin. In the 0.4 mm fraction, there is a small amount (<5%) of rounded quartz, which appears regularly throughout the deposit.

Elemental composition of the organic matter (carbon, nitrogen) and LOI

The carbon (C) and nitrogen (N) contents of the S1 deposit are generally low (0.2–1.6% C and 0.04–0.1% N), with both elements following a similar pattern of variation, showing their highest values in the basal layer with the highest content in silt and clay (unit V) and the lowest in the upper units of the deposit (III, II and I) (Online Resource 1). The LOI follows a similar pattern to C and N. In S1 the highest values (1.0–2.2%) are found in the basal layers (units VI and V) (Fig. 3 and Online Resource 1). From the bottom of the transition layer (unit IV) there is

a progressive decrease in the LOI values (1.3–0.3%) until the top of the deposit is reached (0.3%). The upper units are the richest in sand and have the lowest LOI content. The LOI for S4 shows a similar trend to S1, albeit with slightly higher values. In units VI and V, the values range from 4.2% to 2.3% and are associated with layers with the highest amount of silt and clay (Fig. 3). In the transition layer (unit IV) the LOI is between 2.1% and 1.2%. The lowest LOI values (0.8–0.3%) are found in units III, II and I, coinciding with the sandier layers.

Elemental composition of the mineral fraction: Si, Al, Fe, Ti, K, Ca, Na, Zr and Sr

Seven major chemical elements of the inorganic or mineral fraction (Si, Al, Fe, Ti, K, Ca, Na) and two lithogenic trace elements (Sr, Zr) were analysed in S1 (Fig. 3 and Online Resource 1). The elements Al, Fe, Ti, Ca, Na, Sr and Zr present a similar pattern: low concentration and similar variations in the upper sandy layers (unit IV to I) and maximums in the basal silt–clay layers enriched with iron oxides (units VI and V). These elements present a strong positive correlation with the silt–clay fraction ($r = 0.90$, 0.80, 0.85, 0.97, 0.94, 0.95, 0.68, respectively). However, Si and K follow an inverse pattern as they show a negative correlation with the silt–clay content (Si $r = -0.95$; K $r = -0.58$).

Mineralogical composition

The samples analysed in S1 are dominated by quartz, potassium feldspar (microcline) and plagioclase (albite), with a low abundance of micas (Online Resource 2). Due to the fact that all of the samples have a high sand content, they are also rich in quartz, which is predominant in the upper units (III, II and I) (Online Resource 2a), while in the basal units (VI and V), microcline and plagioclase are more abundant (Online Resource 2b). Feldspars are the result of the physical fragmentation of granite.

Discussion

Evolution of the pedosedimentary deposits S1 and S4

The granulometric and mineralogical data, elemental composition, and stratigraphic features of S1 and S4 made it possible to distinguish three phases of environmental change: granite weathering, continental soil formation and erosion, and coastal sedimentation.

Granite weathering facies

In unit VI of S1 and S4, the granulometric and morphological composition (presence of angular quartz and feldspar gravels in a fine-grained, plastic and adherent matrix with iron oxides), mineralogy (occurrence of plagioclase and micas, with quartz and K-feldspars as dominant minerals) and concentration of major elements, such as Ca, or trace elements, such as Sr, suggest that this unit is the result of in situ weathering of the granite rock substrate (Taboada and Garćia 1999).

Soil formation and erosion: continental facies

Unit V is a dark brown palaeosoil developed from a colluvial sediment, the source of which is the weathered granites. The occurrence of angular granite fragments in the gravels of the soil suggests a continuous supply from a nearby area of weathered granites. The presence of a palaeosoil indicates that it developed under stable landscape conditions. The abundance of gravels and the high content of Ca, Na, C, N and LOI are properties indicative of in situ soil formation (Fig. 3 and Online Resource 1). The properties of this palaeosoil are quite similar to those of other Holocene palaeosoils found in NW Spain, which are characterised by higher values of C, N and LOI than the fossilising upper layers (Costa-Casais et al. 2008, 2012a, b; Martínez-Cortizas et al. 2009). Above unit V, there is a change in the sedimentation represented in unit IV, with a predominance of moderately sorted sands, with a mean grain-size of 0.4 mm, and less than 1% of gravels. There is also a progressive increase in Si towards the upper part, while C and LOI content decreases (Fig. 3). Sedimentary and geochemical properties point to the erosion of the underlying unit V as the main sediment source, although some supply from weathered granites from nearby areas could be maintained. The upwards increase in sand content and its properties, which are identical to the upper coastal layers described below, point to coastal processes as the main sedimentary process for units IV to I, although the occurrence of a small amount of granite gravels suggests that there was a phase of instability in the landscape.

The occurrence of ceramic fragments attributed to the Neolithic (Chao-Álvarez 2015), and, especially, charcoals are evidence of human presence. It is noteworthy that both deposits are located in close proximity to two funerary tumuli. The content in organic matter and the amount of silt–clay fractions decrease upwards, as do other geochemical markers, such as Sr and Ca. This would suggest that, after the deposition of sands, there was a period of stability without sediment supply and enough time for soil development. Unit IV shows evidence of truncation, with small cracks infilled with the sand of the upper layers interpreted as probable root marks.

Coastal facies

The upper layers (units III, II and I) are homogeneous and are composed of moderately well-sorted medium sands (mean grain-size 0.4 mm), mostly composed of quartz but with some potassium feldspars (Online Resource 2a). These layers have the highest amount of Si, while Ca, Na, Sr and LOI values decrease (lowest values of the entire column) (Fig. 3). In the upper sections of both columns (40 cm in S1 and 60 cm in S4) there is evidence of biogenic carbonates (small shell fragments). Although these fragments are too small to make a clear identification, given the granulometry of the sands, it was possible to distinguish that they are marine bivalves. The shoals in which Areoso Island is located are surrounded by steep submarine scarps and are structurally disconnected from the continent. Therefore, there is a lack of sedimentary supply from rivers or other continental sources (Blanco-Chao et al 2020). The only available sources of sand supply to the beach were the sandy subtidal bodies and the erosion of the continental sedimentary deposits on the island itself. Most of the sedimentary mineral particles are angular or subrounded, indicating poor transport from their area of origin. The lack of reworking points to the erosion of the continental facies described above (units VI and V) as the main source of sediment nourishing the beach. Only in the 0.4 mm fraction is there a small amount of rounded quartz, which appears regularly throughout the deposit and can be interpreted as originating from a different source (probably older and more distant), that has been incorporated into the sediments. The bottom of these layers is at an elevation of 1.8 m (a.p.m.s.l.) in S1 and 1.3 m in S4, and the top (the present beach) is between 2.3 and 2.5 m (a.p.m.s.l.), which corresponds to the present Maximum Astronomical High Tide (MAHT) (Fig. 3).

The differences between the three units are mainly related to evidence of incipient pedogenesis. Unit II is darker and shows a better structure that the underlying unit III, and in S1 there are some rounded and subrounded granite gravels. Both in S1 and S4, there are some subrounded ceramic fragments, the cultural origin of which has not been possible to determine, due to the lack of decoration or any other property that would allow archaeologists to identify the cultural stage. The uppermost layer (unit I) is the top of both deposits and shows slight features of pedogenesis.

The properties of the upper units point to coastal sedimentary processes, corresponding to the establishment of a beach-dune system like the present one. Units III to I are within the range of wave action, and no evidence of higher sea-level has been found on the island. The formation of units III to I had enough time to develop a beach after the sea-level reached its present position. The occurrence of episodes of pedogenesis could, then, be related to variations in

the wave energy regime and changes in the position of the dune fronts or beach profiles.

Chronostratigraphic reconstruction: holocene transgression

Three different facies have been identified from the sedimentary record of the studied deposits (continental, transitional and coastal), thus making it possible to reconstruct the Late Holocene sea-level rise.

The base of the pedostratigraphic record of S1 and S4 (units VI–V) corresponds to a continental environment with a sea-level lower than that of the present. Weathered granite (unit VI) would have developed before 6.0 kyr BP, according to the earliest datings (6398–6285 cal yr BP in S4 and 5840–5610 cal yr BP in S1), under warm and wet conditions during the Holocene Climatic Optimum (ca. 7.0–5.5 kyr BP) (Kalis et al. 2003) (Fig. 4). This phase was followed by another dominated by the erosion of products of weathering, which were transported and sedimented, leading to the exhumation of the rock substrate in those areas at higher elevations on the island. This process of rock exhumation, erosion and transport has been documented in other areas of the NW Iberian Peninsula and has been related not only with specific environmental conditions, such as intense rains, but also with increased human activity (Costa-Casais et al. 2012a; Martínez-Cortizas et al. 2009).

The Holocene Climatic Optimum ended approximately at 5.5 kyr BP with the beginning of the Neoglaciation, a different climatic phase with temperatures up to 2 °C lower than those of the present. This lasted until 3.5 kyr BP (Martínez-Cortizas and Pérez-Alberti 1999). The date of 4825–4570 cal yr BP obtained in the middle of the unit V in S1 can be included in this cold and humid climatic context (Magny et al. 2006; van Geel et al. 2000; Lal et al. 2007), coincident with the most intense Neolithic occupation of the island. The chronology of the funerary construction period in Areoso has been ascribed to the third millennium BC (Rey García 2011). Occupation took place at that time when the sea-level was still low, the island was larger and the palaeosoil of unit V was extended over a wider area. The intense anthropic impact with the construction of the tumuli in the highest and most visible sectors of the island increased instability, as shown by the truncation of the palaeosoil (unit V) at the top.

Unit IV (transitional) shows a change in the environment with the sedimentation of increasing amount of sands. The accumulation of charcoals and archaeological pottery at the base of unit IV suggests that anthropic pressure was still a factor of instability on the landscape. Precisely, the presence of charcoals shows the use of fire, which would have caused accelerated soil erosion via the elimination of protective vegetation cover, with the direct result of exposing the mineral soil to erosion (Costa-Casais et al. 2012b). Episodes of accelerated deforestation are usually coincident with periods of increased human pressure and cultural changes reflected in many areas of Europe, such as the Neolithic expansion of agriculture and grazing around 6.0 kyr BP, the Bronze Age/
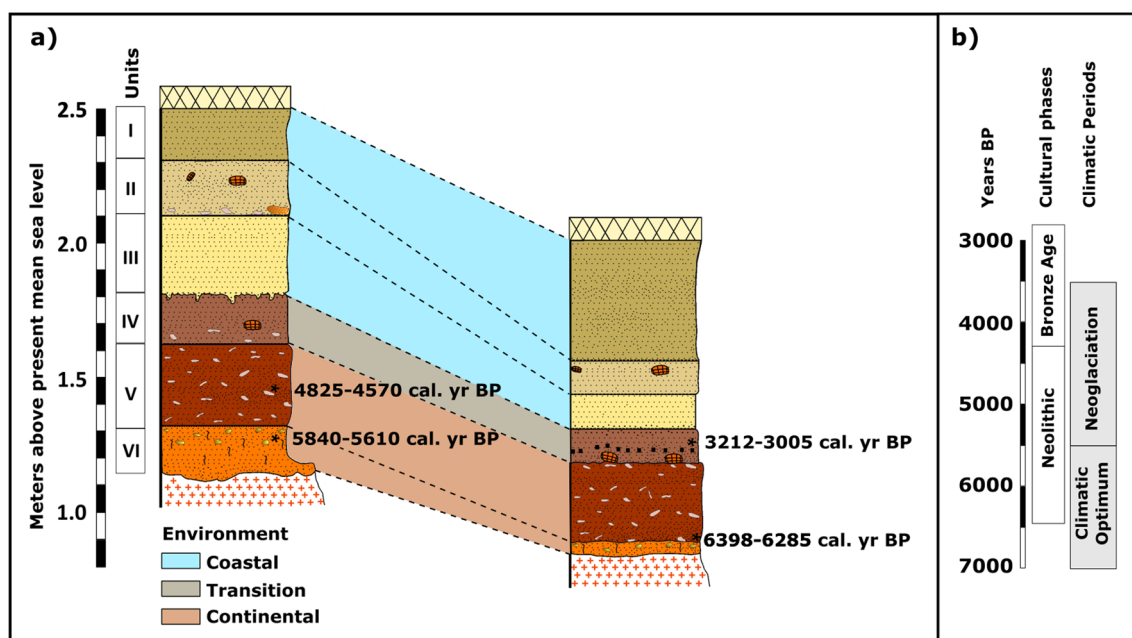
Fig. 4 **a** Synthesis of the main sedimentological environments. **b** Cultural phases and climatic periods between 7000 and 3000 yr BP

Iron Age transition around 3.0 kyr BP and the 1.7–1.5 kyr BP Roman/Germanic shift (Tinner et al. 1999; Mighall et al. 2006).

The upper part of unit IV, just above the accumulation of pottery remnants and charcoals deposited after 3212–3005 cal. yr BP, shows a change in the sedimentary environment with a shift to coastal processes. The base of the upper section of the unit is at an elevation of 1.25 m a.p.m.s.l. in S4 and 1.8 m a.p.m.s.l. in S1, which correspond to the present-day elevation between mean neap and mean spring high water levels and is, therefore, in equilibrium with a sea-level like that of the present day. The timing agrees with previous studies carried out on the coast of the NW of the Iberian Peninsula, stating that the present-day sea-level was not reached before 4.0–3.5 kyr BP (Bao et al. 2007; Costas et al. 2009; González-Villanueva et al. 2015). Therefore, unit IV represents the first influence of coastal processes in the studied deposits. The occurrence of root cracks at the top of unit IV would be indicative of a period of plant colonisation after the first episode of beach sedimentation.

The upper units (III, II and I) represent the establishment of a beach after 3212–3005 cal. yr BP, which has remained until today. No evidence of significant change in sedimentation has been observed since that date. This fact could be interpreted as a stabilization of the sea-level, although the absence of dating in levels III to I does not allow us to reject the existence of a hiatus between units IV and III. The low degree of variability in the granulometry of the upper sandy layers, and in the incipient features of soil development, shows that both flanks of the beach were probably subjected to changes in wave energy, beach profile and dune development. The small difference (40–50 cm) in the relative elevation of the units with respect to the present mean sea-level is probably a consequence of the slightly different wave environment in the eastern and western flanks of the island, strongly influenced by the propagation of open ocean waves inside the ria and by the local north winds (Blanco-Chao et al. 2020). The occurrence of ceramic fragments close to the upper layers, with no (or very little) reworking, is probably the consequence of recent erosion of the archaeological sites, a well-documented process during the twentieth and twenty-first centuries (Blanco-Chao et al. 2020), as a modern coin from 1986 was also found in the same layer, what suggest that units II and I are probably very recent.

Final remarks

The two pedosedimentary deposits analysed make it possible to reconstruct the evolution of Areoso Island over the last 6000 years. The physical and chemical properties of S1 and S4, located on opposite flanks of the island, reveal that they have similar formation facies at a similar elevation related to the present mean sea-level. The pedosedimentary units reveal a change from a full continental environment to the establishment of a beach system.

A phase of rock weathering took place on both flanks of the island, followed by an erosive phase caused by both climatic factors and human pressure on the landscape. The continental facies shows low sea levels up to at least 4.8 kyr BP. After 3.2 kyr BP, a phase of coastal sedimentation began and a beach system, similar to the present context, was formed.

Thus, the geomorphological processes in the Middle and Late Holocene on Areoso Island have been influenced by climatic conditions, sea-level change and anthropogenic activity.

Declarations

References

Alonso A, Pagés JL (2010) Evolución del nivel del mar durante el Holoceno en el noroeste de la Península Ibérica. Rev Soc Geol Esp 23:157–167

Álvarez-Alonso D, Pardo JFJ, Carral P, Flor-Blanco G, Flor G, Iriarte-Chiapusso MJ, Kehl M, Klasen N, Maestro A, Rodríguez Asensio A, Weniger GC (2020) At the edge of the Cantabrian sea. New data on the Pleistocene and Holocene archaeological open-air site of Banugues (Gozon, Asturias, Spain): palaeogeography, geoarchaeology and geochronology. Quat Int 566:284–302. https://doi.org/10.1016/j.quaint.2020.04.025

Andrade A, Rubio B, Rey D, Álvarez-Iglesias P, Bernabeu AM, Vilas F (2011) Palaeoclimatic changes in the NW Iberian Peninsula during the last 3000 years inferred from diagenetic proxies in the Ría de Muros sedimentary record. Clim Res 48:247–259. https://doi.org/10.3354/cr00992

Andrade A, Rubio B, Rey D, Álvarez-Iglesias P, Bernabeu AM, Fedi M (2014) Environmental changes at the inner sector of Ría de Muros (NW Spain) during Middle to Late Holocene. Estuar Coast Shelf Sci 136:91–101. https://doi.org/10.1016/j.ecss.2013.11.005

Bao R, Alonso A, Delgado C, Pagés JL (2007) Identification of the main driving mechanisms in the evolution of a small coastal wetland (Traba, Galicia, NW Spain) since its origin 5700 cal yr BP. Palaeogeogr Palaeocl 247(3–4):296–312. https://doi.org/10.1016/j.palaeo.2006.10.019

Benjamin J, Rovere A, Fontana A, Furlani S, Vacchi M, Inglis RH, Galili E, Antonioli F, Sivan D, Miko S, Mourtzas N, Felja I, Meredith-Williams M, Goodman-Tchernov B, Kolaiti E, Anzidei M, Gehrels R (2017) Late Quaternary sea-level changes and early human societies in the central and eastern Mediterranean Basin: an interdisciplinary review. Quat Int 449:29–57. https://doi.org/10.1016/j.quaint.2017.06.025

Blanco-Chao R, Costa-Casais M, Martínez-Cortizas A, Pérez-Alberti A, Trenhaile AS (2003) Evolution and inheritance of a rock coast: western Galicia, northwestern Spain. Earth Surf Proc Land 28(7):757–775. https://doi.org/10.1002/esp.496

Blanco-Chao R, Costa-Casais M, Cajade-Pascual D, Gómez-Rey G (2019) Coastal retreat and sedimentation during the last 3000 years. Atlantic coast of NW Spain. J Mar Sci Eng 7(10):331. https://doi.org/10.3390/jmse7100331

Blanco-Chao R, Cajade-Pascual D, Costa-Casais M (2020) Rotation, sedimentary deficit and erosion of a trailing spit inside ria of Arousa (NW Spain). Sci Total Environ 749:141480. https://doi.org/10.1016/j.scitotenv.2020.141480

Blott SJ, Pye K (2001) GRADISTAT: a grain size distribution and statistics package for the analysis of unconsolidated sediments. Earth Surf Proc Land 26(11):1237–1248. https://doi.org/10.1002/esp.261

Cartelle V, García-Moreiras I, Martínez-Carreño N, Sobrino CM, García-Gil S (2022) The role of antecedent morphology and changing sediment sources in the postglacial palaeogeographical evolution of an incised valley: The sedimentary record of the Ría de Arousa (NW Iberia). Global Planet Change 208:103727. https://doi.org/10.1016/j.gloplacha.2021.103727

Chao-Álvarez J (2015) Sondaxes arqueolóxicas valorativas e labores de conservación no illote de Guidoiro Areoso (Illa de Arousa–Pontevedra). Technical report. Consellería de Cultura, Xunta de Galicia

Cheburkin AK, Shotyk W (1996) An energy dispersive miniprobe multieleme analyzer (EMMA) for direct analysis of Pb and other trace elements in peats. Fresenius J Anal Chem 354:688–691. https://doi.org/10.1007/s0021663540688

Costa-Casais M, Martínez-Cortizas A, Kaal J, Ferro-Vázquez C, Criado-Boado F (2008) Depositos coluviales holocenos del NO peninsular: geoarchivos para la reconstruccion de la dinámica geomorfologica. In: Benavente J, Gracia FJ (eds) Trabajos de Geomorfologia en España 2006 2008. X Reunión Nacional de Geomorfología. SEG, Cádiz, pp 83–86

Costa-Casais M, Martínez-Cortizas A, Kaal J, Caetano Alves MI, Criado-Boado F (2012a) Reconstructing Holocene evolution in the archaeological site of Campo Lameiro (NW Spain): an interdisciplinary approach to geoarchaeology. In: Almeida AC, Bettencourt AMS, Moura D, Monteiro-Rodrigues S, Caetano Alves MI (eds) Environmental changes and human. Interaction along the western Atlantic edge. APEQ, Coimbra, pp 51–69

Costa-Casais M, Martínez-Cortizas A, Pontevedra-Pombal X, Berasategui Vinagre I, Ferro-Vázquez C, Rodríguez Racedo J (2012b) Evolución holocena do sector costeiro de Punta dos Pericos (Ribeira, A Coruña). In: Fábregas-Válcarce R, Rodríguez-Rellán C (eds) A Arte Rupestre no Norte do Barbanza. Andavira Editora, Santiago de Compostela, pp 153–172

Costas S, Sobrino CM, Alejo I, Pérez-Arlucea M (2009) Holocene evolution of a rock-bounded barrier-lagoon system, Cíes Islands, northwest Iberia. Earth Surf Proc Land 34(11):1575–1586. https://doi.org/10.1002/esp.1849

David O, Penaud A, Vidal M, Fersi W, Lambert C, Goubert E, Herlédan M, Stéphan P, Pailler Y, Bourillet JF, Baltzer A (2022) Sedimentological and palynological records since 10 ka BP along a proximal-distal gradient on the Armorican shelf (NW France). Quat Sci Rev 293:107678. https://doi.org/10.1016/j.quascirev.2022.107678

Erlandson JM (2012) As the world warms: rising seas, coastal archaeology, and the erosion of maritime history. J Coast Conserv 16:137–142. https://doi.org/10.1007/s11852-010-0104-5

FAO (2009) Guía para la descripción de suelos. Organización de las Naciones Unidas para la agricultura y la alimentación, Rome

Feal-Pérez A, Blanco-Chao R, Ferro-Vázquez C, Martínez-Cortizas A, Costa-Casais M (2014) Late-Holocene storm imprint in a coastal sedimentary sequence (Northwest Iberian coast). Holocene 24:477–488. https://doi.org/10.1177/095968361352025

Fitzpatrick SM, Rick TC, Erlandson JM (2015) Recent progress, trends, and developments in island and coastal archaeology. J Isl Coast Archaeol 10(1):3–27. https://doi.org/10.1080/15564894.2015.1013647

Folk RL, Ward WC (1957) Brazos River bar [Texas]; a study in the significance of grain size parameters. J Sediment Res 27(1):3–26. https://doi.org/10.1306/74D70646-2B21-11D7-8648000102C1865D

Fruergaard M, Andersen TJ, Nielsen LH, Madsen AT, Johannessen PN, Murray AS, Kirkegaard L, Pejrup M (2011) Punctuated sediment record resulting from channel migration in a shallow sand-dominated micro-tidal lagoon, Northern Wadden Sea, Denmark. Mar Geol 280(1–4):91–104. https://doi.org/10.1016/j.margeo.2010.12.003

García-Artola A, Stéphan P, Cearreta A, Kopp RE, Khan NS, Horton BP (2018) Holocene sea-level database from the Atlantic coast of Europe. Quat Sci Rev 196:177–192. https://doi.org/10.1016/j.quascirev.2018.07.031

García-Moreiras I, Cartelle V, García-Gil S, Muñoz Sobrino C (2019) First high-resolution multi-proxy palaeoenvironmental record of the Late Glacial to Early Holocene transition in the Ría de Arousa (Atlantic margin of NW Iberia). Quat Sci Rev 215:308–321. https://doi.org/10.1016/j.quascirev.2019.05.016

Gómez-Orellana L, Ramil-Rego P, da Costa JF, Muñoz Sobrino C (2021) Holocene environmental change on the Atlantic coast of NW Iberia as inferred from the Ponzos wetland sequence. Boreas 50(4):1131–1145. https://doi.org/10.1111/bor.12535

González-Villanueva R, Pérez-Arlucea M, Costas S, Bao R, Otero XL, Goble R (2015) 8000 years of environmental evolution of barrier–lagoon systems emplaced in coastal embayments (NW Iberia). Holocene 25:1786–1801. https://doi.org/10.1177/0959683615591351

Granja H, Gómez-Orellana L, Costa AL, Morais R, Oliveira C, Ramil-Rego P, Pinho JL (2022) Holocene evolution of the Cávado estuary (NW Portugal). Quat Int 622:36–50. https://doi.org/10.1016/j.quaint.2022.02.032

Guitián F, Carballas T (1976) Técnicas de Análisis de suelos. Pico Sacro, Santiago de Compostela

Kalis AJ, Merkt J, Wunderlich J (2003) Environmental changes during the Holocene climatic optimum in central Europe—human impact and natural causes. Quat Sci Rev 22(1):33–79. https://doi.org/10.1016/S0277-3791(02)00181-6

Lal D, Largem WG, Walker SG (2007) Climate forcing before, during, and after the 8.2 kyr BP global cooling event. J Earth Syst Sci 116(171):177. https://doi.org/10.1007/s12040-007-0017-3

Lambeck K, Rouby H, Purcell A, Sun Y, Sambridge M (2014) Sea level and global ice volumes from the last glacial maximum to the Holocene. Proc Natl Acad Sci 111:15296–15303. https://doi.org/10.1073/pnas.1411762111

Leorri E, Fatela F, Drago T, Bradley SL, Moreno J, Cearreta A (2013) Lateglacial and Holocene coastal evolution in the Minho estuary (N Portugal): Implications for understanding sea-level changes in Atlantic Iberia. Holocene 23(3):353–363. https://doi.org/10.1177/0959683612460786

López-Romero E, Güimil-Fariña A, Mañana-Borrazás P, Otero Vilariño C, Prieto-Martínez MP, Rey García JM, Vilaseco-Vázquez XI (2015) Ocupación humana y monumentalidad durante la Prehistoria Reciente en el islote de Guidoiro Areoso (Ría de Arousa, Pontevedra): investigaciones en el marco de las dinámicas litorales atlánticas actuales. Trab Prehist 72:353–371. https://doi.org/10.3989/tp.2015.12159

Magny M, Leuzinger U, Bortenschlager S, Haas JN (2006) Tripartite climate reversal in Central Europe 5600–5300 years ago. Quat Res 65:319. https://doi.org/10.1016/j.yqres.2005.06.009

Mañana-Borrazás P, Blanco-Chao R, Bóveda MJ, Cajade-Pascual D, Costa-Casais M, Güimil-Fariña A, López-Romero E, Vázquez-Collazo S, Vilaseco-Vázquez XI (2020) Lo que nos cuenta la marea. Prehistoria en el islote de Guidoiro Areoso (A Illa de Arousa, Galicia) a la luz de las últimas intervenciones. In: Actualidad de la Investigación Arqueológica en España I (2018–2019). Museo Arqueológico Nacional, Madrid, pp 159–176

Martínez-Carreño N, García-Gil S (2017) Reinterpretation of the Quaternary sedimentary infill of the Ría de Vigo, NW Iberian Peninsula, as a compound incised valley. Quat Sci Rev 173:124–144. https://doi.org/10.1016/j.quascirev.2017.08.015

Martínez-Cortizas A, Pérez-Alberti A (1999) Atlas Climático de Galicia. Xunta de Galicia, Santiago de Compostela

Martínez-Cortizas A, Costa-Casais M, López-Sáez JA (2009) Environmental change in NW Iberia between 7000 and 500 cal BC. Quat Int 200(1–2):77–89. https://doi.org/10.1016/j.quaint.2008.07.012

Mighall T, Martínez-Cortizas A, Biester B, Turner SE (2006) Proxy climate and vegetation changes during the last five millennia in NW Iberia: pollen and non-pollen palynomorph data from two ombrotrophic peat bogs in the North Western Iberian Peninsula. Rev Palaeobot Palynol 141:202–223. https://doi.org/10.1016/j.revpalbo.2006.03.013

Muñoz Sobrino C, Cartelle V, Martínez-Carreño N, Ramil-Rego P, García-Gil S (2022) The timing of the postglacial marine transgression in the Ría de Ferrol (NW Iberia): a new multiproxy approach from its sedimentary infill. CATENA 209:105847. https://doi.org/10.1016/j.catena.2021.105847

Rey García JM (2011) Guidoiro Areoso (Illa de Arousa, Pontevedra): un pequeño islote con una intensa ocupación entre el Neolítico Final y la Edad del Bronce. In: Prieto Martínez P, Salanova L (eds) Las comunidades campaniformes en Galicia: cambios sociales en el III y II milenios BC en el NW de la Península Ibérica. Diputación de Pontevedra, Pontevedra, pp 201–210

Sáez A, Carballeira R, Pueyo JJ, Vázquez-Loureiro D, Leira M, Hernández A, Valero-Garcés BL, Bao R (2018) Formation and evolution of back-barrier perched lakes in rocky coasts: an example of a Holocene system in north-west Spain. Sedimentology 65(6):1891–1917. https://doi.org/10.1111/sed.12451

Spanish Port Authority (2017) Informe de datos mareógrafo de Vilagarcía. https://www.puertos.es/es-es. Accessed 15 February 2022

Stuiver M, Reimer PJ, Reimer RW (2021) CALIB 8.2 [WWW program] at http://calib.org. Accessed 10 May 2021

Taboada T, García C (1999) Pseudomorphic transformation of plagioclases during the weathering of granitic rocks in Galicia (NW Spain). CATENA 35(2–4):291–302. https://doi.org/10.1016/S0341-8162(98)00108-8

Tinner W, Hubschmid P, Wehrli M, Ammann B, Conedera M (1999) Long term forest fire ecology and dynamics in southern Switzerland. J Ecol 87:273–289. https://doi.org/10.1046/j.1365-2745.1999.00346.x

Urrutia MM, García-Rodeja E, Macías F (1989) Determinación del pH en suelos de carga variable de Galicia. An Edaf Agrob 48:219–228

van Geel B, Heusser CJ, Rensen H, Schuurmans CJE (2000) Climatic change in Chile at around 2700 BP and global evidence for solar forcing: a hypothesis. Holocene 10(5):659–664. https://doi.org/10.1191/09596830094

Wentworth CK (1922) A scale of grade and class terms for clastic sediments. J Geol 30:377–392

Publisher's Note Springer Nature remains neutral with regard to jurisdictional claims in published maps and institutional affiliations.